THE JÜLICH DOUBLE-MONOCHROMATOR SYSTEM

J. Reich, C. Mayer-Böricke, S. Martin
Institut für Kernphysik der Kernforschungsanlage Jülich, D-517 Jülich, Germany

K.L. Brown
Stanford Linear Accelerator Center, Stanford, Ca. 94305, U.S.A.

F.E. Johnson
Varian Associates, Radiation Division, Palo Alto, Ca. 94303, U.S.A.

ABSTRACT

The Jülich double-monochromator system has been brought into operation at the Jülich Isochronous Cyclotron. The results of the ray tracing calculations as well as the tests with the cyclotron beam show that it has a momentum resolution power $R = p_0/\Delta p_{FWHM} = 20000$ and a transmission of about 2 % for 1 mm slit-width settings at the entrance and the exit of the system. These values are obtained for a horizontal and a vertical emittance of 20 and 25 mm·mrad, respectively, and a momentum bin width of 1.5/1000 of the cyclotron beam.

INTRODUCTION

The external beam of the Jülich Isochronous Cyclotron has an energy resolution of 3/1000. When using this beam (up to 180 MeV-α-particles) this energy resolution is sufficient for some nuclear-reaction experiments with light nuclei, which have comparatively large energy spacings between levels. However, the above resolution means 300 keV energy width for a 100 MeV-α-particle beam. Since the level distance in medium weight and heavier nuclei is generally smaller than 300 keV even in the vicinity of the ground state, the resolution of the primary cyclotron beam is not sufficient to study nuclear reactions in this region of nuclei. Therefore an external analysing system is needed to improve the energy resolution. At the time of its initial design the analysing system had to fit into the existing limitations imposed by the cyclotron building. Both requirements - a high resolving power and the fit of the apparatus into the special room limitations - could be fulfilled by the double-monochromator system described below.

THEORETICAL BASIS FOR THE DESIGN

A general equation for the first-order momentum resolving power of a static-magnetic beam transport system possessing median plane symmetry has been derived by K.L. Brown [1,2]. For point-to-point imaging the first-order momentum resolving power R_1 is defined as the ratio of the momentum dispersion at the image plane to the total image size. Thus, if $2x_o$ is the total source size, then

$$R_1 = p_o/\Delta\, p_{FWHM} = \left| \frac{d_x(t)}{2x_o\, c_x(t)} \right| = \frac{1}{2x_o} \left| \int_o^t s_x(\tau) h(\tau) d\tau \right| \quad (1)$$

where $h(\tau)d\tau = d\alpha$ is the differential angle of bend of the central trajectory of the optical system, $c_x(t)$ is the first-order magnification at the image plane, τ is the distance measured along the central trajectory from the origin and $\tau = t$ is the location of the image plane. If we consider a particle originating at the source ($\tau = 0$) with $x_o = 0$, an angle θ_o with respect to the direction of the central trajectory in the midplane and $\delta = \Delta p/p_o = 0$, the first-order equation of its trajectory is

$$x(\tau) = s_x(\tau)\theta_o \quad (2)$$

This defines the quantity $s_x(\tau)$ and equation (1) can be written in the form

$$R_1 = \frac{1}{2x_o\theta_o} \left| \int_o^t \frac{B \cdot x(\tau) d\tau}{(B\rho)} \right| = \frac{1}{2x_o\theta_o} \frac{1}{B\rho} \left| \int_o^t BdA \right| \quad (3)$$

where $\int BdA$ is the magnetic flux enclosed between the central trajectory and the trajectory described by equation (2), and $B\rho$ is the magnetic rigidity of the central trajectory. From equation (3) the resolving power may be defined as the magnetic flux enclosed per unit phase space area ($2x_o\theta_o$) and per unit momentum ($B\rho$) of the central ray. The above equations may be used as a guide toward achieving the required resolving power.

For a double-monochromator design using two bending magnets with homogeneous fields and having point symmetry with respect to the center, equation (1) may be integrated and expressed in the following compact form

$$2x_oR_1 = \frac{2}{M_c} [\ell_3(\sin\alpha + \tan\beta_2(1-\cos\alpha)) + \rho(1-\cos\alpha)] \quad (4)$$

where M_c is the magnification at the horizontal crossover in the center of the system, ℓ_3 is the distance from

the exit of the first magnet to the image point at the center, β_2 is the angle of rotation of the exit face of the magnet, α is the angle of deflection of the central trajectory and ρ is the radius of curvature of the central trajectory.

FIRST AND SECOND ORDER DESIGN

In the Jülich case the analysis of equation (4) led to the incorporation of quadrupole singlets in the design, in order to optimize the resolving power within the restricted space available. The final design came up with a double-monochromator system (see fig. 1) which is pointsymetric to the central slit IS. Each half of the

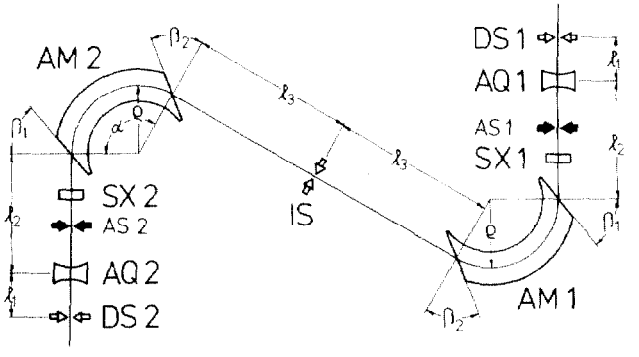

Fig.1 Lay out of the double-monochromator system. AS1/2: slits for the single achromatic mode

system gives half the resolving power of the total system. There is a double focus at the central slit as well as at the exit slit DS2. Each of the two halfs consists of a 120°-analysing magnet AM, a quadrupole-singlet lense AQ and a sextupole lense SX. The analysing magnets have homogeneous field with radially defocusing β-angles at entrance and exit. The quadrupole singlet lenses are radially defocusing as well.

Inserting the relevant parameters of table 1 into equation (4) the first-order resolving power of the system can be calculated to be 36000 for a source size of $2x_o$ = 1 mm. This is one of the highest design objectives for a first-order resolving power incorporated in a beam transport system to date. Clearly, second order effects must be considered for such high resolving powers. For second-order correction the effective fringe-field boundaries of the analysing magnets were originally

designed to have convex curvatures on the entrance of AM1 and the exit of AM2 and to be straight on the exit of AM1 and the entrance of AM2. However, fabricational tolerances calculated during the manufacturing stage resulted in a decision to have four straight boundaries and two adjustable sextupole lenses for introducing the second order corrections. This alternative proved to be more flexible because the tunig of the sextupoles can account for the final performance of the system and for slight variation of the field form over the tuning range of the system. When correcting the $(x|\theta^2)$ aberration, the main aberration of concern, the resolving power R_2, calculated to second order, was 25000 with a transmission T_2 of 2 % for 1 mm slit-width settings at the entrance and exit of the system. This calculation was based on a horizontal and a vertical emittance of 20 and 25 mm·mrad, respectively, and a momentum-bin width of 1.5/1000 of the cyclotron beam.

All first- and second-order calculations throughout the project were carried out with the program TRANSPORT [2]. Fig. 2 shows the horizontal and vertical beam envelopes of the Jülich double-monochromator design (1)

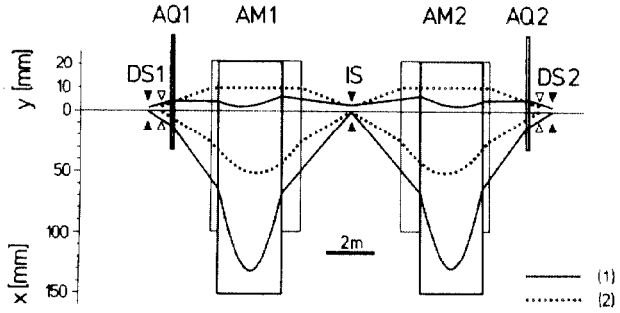

Fig.2 Beam envelopes for the Jülich design (1) in comparison to a more conventional design (2)

in comparison to a more conventional design (2). This second design with much larger analysing magnets has no quadrupole singlets but is double focusing at the middle and the exit slits and would fit into the available space. For this design the flux enclosed within the horizontal beam envelope is much smaller and correspondingly the system has less first-order resolving power.

Table 1 Parameters of the two designs related to fig. 2

Design	ℓ_3 (m)	ρ (m)	β_2	α	M_c	R_1	R_2	T_2 (%)
(1)	2.89	1.22	51.25°	120°	0.54	36000	25000	2
(2)	2.06	1.75	41.52°	120°	1.00	14300	12700	-

MAGNET DESIGN, MANUFACTURING STAGE AND FIELD MAPPING

The analysing magnets are H-type magnets with an air gap of 4.3 cm. The design aim was to achieve a field-form stability in terms of the variation of the effective magnetic path length $\Delta L/L_{eff}$ of better than $5 \cdot 10^{-4}$ in the dynamic range of 3.2 to 16.75 kG. Therefore the edge of the poles has an approximate Rogowski contour. At a distance of 5 gap widths from the physical pole boundary the fringing field is controlled by field clamps and the reverse flux from the yokes is retained by iron plates. The ratio of pole width to horizontal beam spread measured along the exit- and entrance-pole boundaries is only about 2. This ratio is critical because the ion optical design required large β-angles of more than 50° which initiate highly peaked inner pole-face corners. It turned out during the manufacturing stage that because of saturation effects in these pole-face corners the effective fringe-field boundaries were reduced from the design objectives. This difficulty was overcome by using a special iterative procedure for fringe-field shaping [3]. The initial field measurements of the magnetic components made in the manufacturing plant have been checked later at Jülich by a complete field mapping for 4 different main field settings B_0. The achieved field-form stability $\Delta L/L_{eff}$ is better than 10^{-3}. The β-angles are off from the design objectives by about 3/4 of a degree, but the effective fringe field boundaries seen by the beam are straight within $\pm$ 0.15 mm.

RAY TRACING CALCULATIONS

According to the difference between design and performance the lay out of the system has been changed somewhat, namly the object and image distances to the slits DS1 and DS2, respectively, had to be enlarged by 0.23 m. According to this and the mapping data, ray-tracing calculations took place. In the ray-tracing calculation the phase space at the entrance of the system is represented as a 5-dimensional parallelepiped according to the 5 particle coordinates used by TRANSPORT.

The phase space is divided into cells by a 5-dimensional grid. From each cell a ray is integrated through the magnet system for different field representations. At the exit of the system the ray is sorted into a one dimensional grid from which the intensity profile for a given particle coordinate is calculated.

Fig. 3 shows the results for the TRANSPORT-conform representation of the mapping data. The results of TRANSPORT calculations are valid to second order. The results meet the design aim of a momentum resolving power R_2 calculated to second order of 25000 and a transmission of 2 %, both values calculated for 1 mm slit-width settings. The relevant parameters of the performance in comparison to the design related to second order are given in table 2.

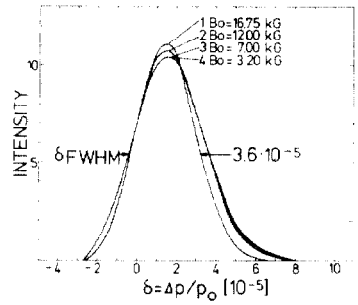

Fig.3 Momentum distributions beyond a 1 mm wide exit slit DS2, calculated to second order for 4 different main field settings B_0

Table 2 Parameters of performance (1) and design (2) related to second-order calculations

No.	β_2	M_c	$R_1/1000$	$R_2/1000$	T_2
(1)	$52.1\pm0.10^\circ$	0.61 ± 0.10	$32.0^{+2.7}_{-1.4}$	$25.0^{+2.8}_{-1.7}$	2.0 ± 0.1
(2)	51.25°	0.54	36.0	25.0	2.0

The errors indicate the width of variation with respect to the mean value, observed for different main field settings B_0 in the dynamic range between 3.20 and 16.75 kG.

EXPERIMENTAL RESULTS

After installation the double-monochromator system was tested with the cyclotron beam. Fig. 4 gives a view of the system as it is now in the cyclotron vault. The test of the described high resolving power is difficult because suitable nuclear resonance reactions for an ex-

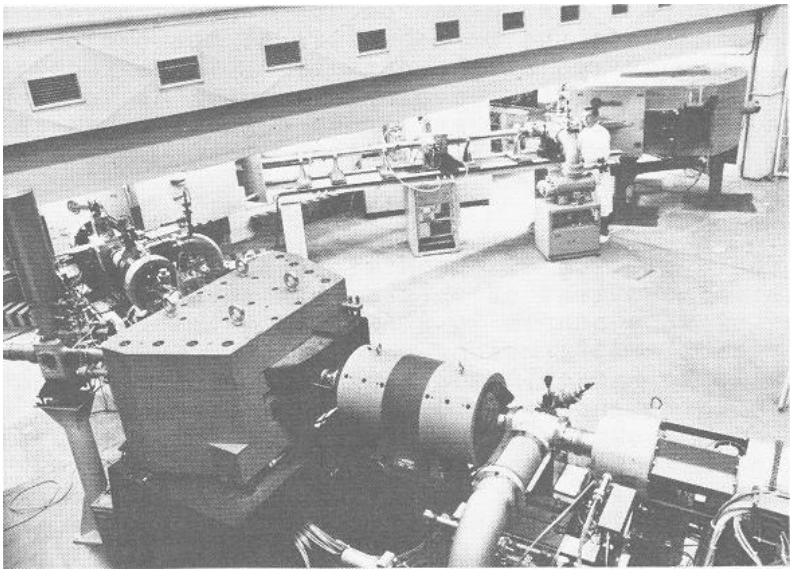

Fig.4 View of the Jülich double-monochromator system in the cyclotron vault

perimental proof are not known in the energy ranges of the JÜlich Isochronous Cyclotron. The test of the resolving power has been made in the following way: According to the described field measurements the first half and the center slit IS of the system were set to give half resolving power of the total system. The horizontal beam profile at the exit slit DS2 of the total system was then measured. The cross points in fig. 5 which represent this profile, are to be compared with a distribution calculated for a bin width $2\delta_{init.} = 9 \cdot 10^{-5}$. Accordingly the resolving power of half the system is larger than 11000. The transmission for 1 mm slit-width

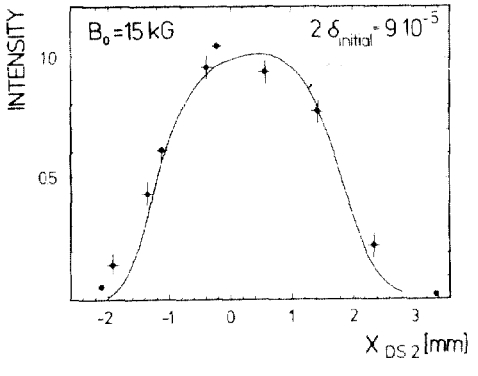

Fig.5 Horizontal beam profile measured at the exit slit DS2 in comparison to a distribution, calculated for $2\delta_{init.} = 9/100000$. For the measurement the first half and the center slit IS of the system were set to give half the resolving power of the total system.

settings during test measurements ranged between 1.5 and 2 % according to the beam quality of the cyclotron beam which was measured at the same time. These results, measurements of the beam envelopes as well as tests of the single-achromatic mode performance showed that the system is working satisfactorily.

ACKNOWLEDGEMENT

The evolution of the design, manufacturing, installation and test of this system involved the contribution of many others in addition to the listed authors. Significant contributions were made by Ch. Rockhold, W. Turnbull, R. Marachin and B.O'Brien at the site of Varian Associates and by W. Gebauer, B. Loorbach, A. Retz and G. Schlienkamp at the Jülich site. The authors wish to thank all other envolved staff members at both sites for their careful work in designing, installing and testing the different components of the system.

REFERENCES

1. K.L. Brown, SLAC 75, (1967)
2. K.L. Brown, S.K. Howry, SLAC 91, (1970)
3. F.E. Johnson, R.A. Marachin, C.T. Rockhold, J. Reich and C. Mayer-Böricke, IEEE Trans NS 18, No 3, 890 (1971)

DISCUSSION

SCHUTTE: In one of your slides you compared your data with the more conventional type. Probably I missed it, but can you compare once again the main features of the more conventional one and your less conventional one?

REICH: The more conventional design has much less first-order resolving power: 14,000 in comparison to our design which has a resolving power of 36,000. This occurs even with the fact that the conventional design has much larger radii of bend and correspondingly much larger magnets. This difference comes from the fact that we use quadrupole singlets to blow up the beam in the analysing magnets according to those equations that I showed in the first slide which are a nice tool to optimize first-order resolving power.